International Journal On Engineering Technology and Sciences – IJETS
ISSN(P): 2349-3968, ISSN (O): 2349-3976
Volume VI, Issue V, May - 2019

CLASSIFICATION OF MELANOMA THICKNESS FROM DERMOSCOPIC IMAGES USING KNN CLASSIFIERS

Thrishna S
PG Scholar
Dept. of Electronics and Communication Engineering
Vimal Jyothi Engineering College
Kannur, Kerala
thrishnasb@gmail.com

D.Anto Sahaya Dhas
Professor
Dept. of Electronics and Communication Engineering
Vimal Jyothi Engineering College
Kannur, Kerala
dr.anto@vjec.ac.in

Abstract

Thickness of the melanoma is the most important factor associated with survival in patients with melanoma. It is most commonly reported as a measurement of depth given in millimeters (mm) and computed by means of pathological examination after a biopsy of the suspected lesion. In order to avoid the use of an invasive method in the estimation of the thickness of melanoma before surgery, we propose a computational image analysis system from dermoscopic images. The proposed feature extraction is based on the clinical findings that correlate certain characteristics present in dermoscopic images and tumor depth. In this paper we are going to identify the thickness of melanoma and then classify the melanoma based on the thickness using KNN classifier and it will provide better classification accuracy than other classification. Two classification methods are proposed first one is the binary classification in which melanomas are classified into thin or thick, and secondly a three-class scheme which is classified in to thin, intermediate, and thick.

1 Introduction

Melanoma is a threat of melanocytes, the cells that produce the shade melanin that colors the skin, hair and eyes. Melanoma that happens on the skin, called cutaneous melanoma, is the most well-known sort of melanoma. It is very much acknowledged that just early location can decrease mortality, since the anticipation of patients with melanoma relies upon the thickness of the tumor at the season of careful treatment. On the off chance that the melanoma is bound to the epidermis, it is an in situ melanoma, reparable by satisfactory evacuation with medical procedure. At the point when the dangerous cells have become through the storm cellar film into the more profound layer of the skin (the dermis), it is known as obtrusive melanoma, whose guess compounds with profundity of intrusion. Breslow file is a technique to gauge the profundity of melanoma attack by methods for neurotic examination after incisional or excisional biopsy of the speculated injury. It is estimated vertically in millimeters from the highest point of the granular layer of the epidermis to its most profound part inside the dermis. It is a significant apparatus in prognosing patients' survival. In addition, it speaks to the primary parameter used to build up the width of careful edges of extraction, just as to choose tolerant for sentinel lymph hub biopsy (SNB). SNB is a surgery used to decide whether malignant growth has spread past an essential tumor into the lymphatic framework. Thusly, estimating the thickness of the melanoma before careful extraction is pivotal to survey the high or generally safe of movement, to guarantee satisfactory extraction edges dodging a second increasingly extreme task and to perform SNB if necessary[1].

In any case, Breslow index can be incorrect determined whether the segment of the extracted tumor isn't made along the thickest part of the tumor. Also, considering that melanoma can possibly be analyzed through non-invasive methodologies as a result of its cutaneous area, a few creators recommend that assurance of Breslow list by non-intrusive strategies, for example, dermoscopy or ultrasonography, would be an incredible development in consistently clinical administration of melanoma. Dermoscopy is a non-intrusive procedure that utilizes light and amplification that permits in vivo representation of morphologic structures in pigmented injuries connected with explicit histologic compositional qualities not generally obvious to the unaided eye, expanding melanoma analytic precision by up to 35%. This method has officially given promising outcomes in Breslow list assurance. A few creators have decided a conceivable connection between tumor thickness and scores acquired with determination strategies from dermoscopic pictures, for example, ABCD or seven point agenda. Be that as it may, the greater part of the works have examined the connection between dermoscopic structures, shading highlights, or even highlights of shape and the profundity of melanoma. In this sense, Argenziano et al. shown that shade arrange, dim blue zones, atypical vascular example, and measurement of more than 1.5 mm permitted expectation of thickness when melanomas were sorted in two gatherings: under 0.76 mm, incorporating into situ (flimsy) melanomas, and more or equivalent than 0.76 mm (thick melanomas). Stante et al. completely affirmed the association between these dermoscopic criteria and histological thickness of melanoma.

In the connection between the watched dermatoscopic discoveries and the histopathological thickness was likewise considered, reasoning that shade organize, light-darker shading, and abnormality are increasingly visit in flimsy melanomas and these discoveries steadily vanish and are supplanted by vascular example, dim blue zones, and white scar-like zones in thick melanomas. In recent decades, computerized dermoscopy image examination systems have been proposed to help the determination of pigmented injuries. However, the issue of characterization of the distinctive types of melanoma concurring its thickness by image analysis represents an extraordinary test for its automatic implementation[2].

Table 1: Stages of melanoma according to thickness

Stage I (thin)	<0.76 mm
Stage II (intermediate)	0.76 mm - 1.5 mm
Stage III (thick	>1.5 mm

To the best of our insight, just a work has tended to this issue, arranging tumors into two classes: slight and thick melanomas. The creators grouped the melanoma profundity by a business programming utilizing 49 features identified with shading, geometry, and surface incorporated in that. 141 images from a private database, extricated by the equipment framework property of the possess organization, were utilized. In this work, we propose a computational image investigation framework to assess the thickness of melanoma from dermoscopic pictures dependent on previously mentioned the clinical discoveries. The dermoscopic pictures were removed from the Interactive Atlas of Dermoscopy, distributed by Edra Medical Publishing New Media. A component extraction is performed motivated by the clinical discoveries, choosing a lot of highlights corresponded with melanoma thickness. The primary inspiration of the proposition is to characterize melanoma thickness without utilizing obtrusive strategies. Taking into account that melanoma thickness is a nonstop factor connected with anticipation (and accordingly with patient survival), distinctive grouping choices can be investigated. We initially investigate the execution in the twofold case, and after that we address the test of a better patient forecast undertaking with three phases of profundity. Along these lines, the target of the paired characterization is to recognize melanomas, incorporating into situ ones, and those with of thickness[4]. The three-class conspire, which, to
the creators' information, has not been recently examined in the writing, approaches the grouping of melanomas thinking about three phases of profundity: , 0.76 mm – 1.5 mm and , i.e., slim, moderate, and thick, separately, agreeing the arrangement proposed in. The characterization execution of a few machine learning techniques is thought about, thinking about three execution measurements and the understanding conceivable outcomes of the got models. An ongoing model consolidating strategic relapse with counterfeit neural systems (Logistic relapse utilizing Initial factors and Product Units, LIPU) is connected to the issue. Its primary favorable position is that it prompts interpretable probabilistic models, keeping up an extensive dimension of exactness. Additionally, we select a lot of ordinal grouping strategies for the three-class issue, which are machine learning calculations that accomplish better execution in multi-class undertakings when there is a requesting connection between the classes, increasing ongoing consideration. Our outcomes demonstrate that LIPU show acquires precise outcomes both for the twofold and three-class renditions of the issue, while ordinal arrangement techniques accomplish a superior harmony between the correctnesses got for all classes in the three-class issue, this managing to increasingly strong conduct in patient diagnosis[5].

2 Proposed Work

In this work, a computational image analysis system to estimate the thickness of melanoma from dermoscopic images based on above mentioned the clinical findings. The dermoscopic images were extracted from the Interactive Atlas of Dermoscopy, published by Edra Medical Publishing New Media. A feature extraction is performed inspired by the clinical findings, selecting a set of features correlated with melanoma thickness. The main motivation of the proposal is to classify melanoma thickness without using invasive methods. Considering that melanoma thickness is a continuous variable correlated with prognosis (and thus with patient survival), different classification options can be explored. We first explore the performance in the binary case, and then we address the challenge of a finer patient prognosis task with three stages of depth. In this way, the objective of the binary classification is to distinguish between melanomas <0.76 mm, including in situ ones, and those with _0.76 mm of thickness. The three-class scheme, which, to the authors knowledge, has not been previously studied in the literature, approaches the classification of melanomas considering three stages of depth: <0.76 mm, 0.76 mm – 1.5 mm and >1.5 mm, i.e. thin, intermediate, and thick, respectively, according the classification proposed. The classification performance of several machine learning methods is compared, considering three performance metrics and the interpretation possibilities of the obtained models. The classification is based on KNN classifier, compared to other classifers KNN has better performance, high accuracy, and high precision[8]

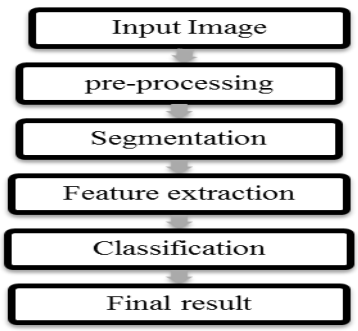

Figure 1: Block diagram

2.1 Preprocessing

From the input RGB image, first extract gray level features from the input image by converting the image to gray

$$Gray = 0.2989*R + 0.5870*G + 0.1140*B$$

is used to convert RGB to grey scale. Where, R indicates the red intensity channel, G green intensity channel and B is the

Figure 2: RGB color image

In Gray scale digital image the value of each pixel is a single sample, it carries only intensity information. Gray scale images are different from one-bit bi-tonal black-and-white images, computer imaging are images with only the two colors, black, and white (also called bi-level or binary images). It have different shades of gray in between, so is also called monochromatic,

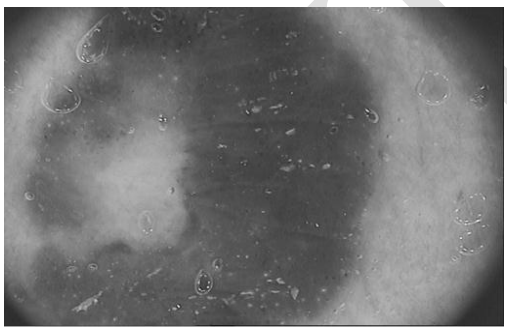

Figure 3: Gray scale image

2.2 Segmentation

After preprocessing the next step is to segment the region of interest. This can be done by converting the image into binary. Since the intensity of the cancer area will be less compared to the intensity of the skin color. so a very low threshold can be used to determines the correct mask for the segmented region of interest.

2.3 Feature Extraction

After segmentation next is to extract the features for classifying next stages. Each stages of cancer will have variations in features. And this different features combine to a single vector. Different features includes

a. Shape features,
b. Color features,
c. Pigment network features,
d. Texture features.

2.3.1.Shape Features

If a diameter of more than 15 mm was more frequent in melanomas with >0.76mm of thickness, and one of the most frequent criterion in thin melanomas was based on asymmetry in two axes. To calculate these criteria, compute area (x1), as number of pixels inside the lesion border, eccentricity (x2), as circularity measure, perimeter (x3), and major axis of the lesion (x4). Eccentricity = $\sqrt{1-\frac{b^2}{a^2}}$ were and are the major and the minor axes of the ellipse that has the same second-moments as the region resulting from the lesion segmentation. A ellipse whose eccentricity is zero is a circle. Eccentricity can be considered a special case of asymmetry.

.3.1. *Color Features*

The more discriminative structure in the melanoma thickness estimation are: pigment network, blue-gray veil, vascular pattern and white scar-like areas. These structures are associated with different colors: pigment network is associated with black and brown, vascular pattern with red color, as the name suggests, blue-gray veil with blue and gray colors, and white scar-like areas with white. Light brown color was more frequent in thin melanomas (<0.76mm), color features play an important role in the depth of melanoma estimation. Here two color feature sets are computed, the first one is related to the six colors assessed in the pigmented lesions, and the second one related to statistics computed over the color of the whole lesion. The first feature set having six main colors black, dark brown, light brown, blue-gray, red, and white to represents the lesion. The different colors appear depending on how deeply in the skin the melanina is located: melanin appears black when it is located in the stratum corneum and upper epidermis. Deeper in the epidermis, it appears brown. In the dermis, melanin appears either gray or blue. Red is associated with dilation of blood vessels and white with regression and/or scaring. Thus, we propose to segment each lesion into their constituting colors. The palette was used to extract the color regions of the lesions from the patches according to a nearest neighbor approach. In each pixel of the image was assigned to the color patch that minimized its Euclidean distance in the RGB color space. In this paper, CIE L*a*b color space,

developed by International Commission on Illumination (CIE), is used, because, unlike RGB, it is a approximately perceptually uniform color space. From this color identification, seven features are extracted. Six descriptors(x5-x10) that represent the percentage of the lesion area classified as these colors. And one more (x11) that represents the number of colors that each lesion presents, criterion established by Silva et al., taking into account in this case that a color must cover at least 1% of the lesion to be counted. Moreover, color of whole lesions were quantified by four Statistics (mean, standard deviation,SD , kurtosis, Ku, and skewness,Sk) over the three channels of two color spaces: RGB and CIELab , i.e., R, G, B, L, a , b and (obtaining 24 additional color features, x12 x34)[10].

2.3.3. Pigment Network Features

The pigment network is a more cited discriminative feature. Its occurrence inversely correlates with melanoma thickness. Due to its importance, we extract specific features derived from pigment network detection. A pigment network is defined as a regular grid of brownish lines over a diffuse light-brown background. Our aim is to seek the 'holes' of the network. The first step is to apply a top hat filter over the channel of lightness L of CIELab color space. Top hat transform extracts objects brighter than their surroundings. After a thresholding by Otsu's method, a binary image with areas that could possibly belong to a pigment network is obtained. In order to remove those wrongly detected areas, we apply the two conditions relative to area size and color To visualize the detected pigment network, a graph, whose nodes are centers of the detected holes belonging to the pigment network, is created. Nodes within a maximum distance threshold, set to 2.5 times the average diameter of holes, are connected together. To detect lesion presented in pigment network, compute the density ratio:

$$\text{Density} = \frac{|E|}{|v|\log(Lesion\ Size)} \qquad (1)$$

To normalize the ratio $|E|/|V|$from this pigment network detection, 3 features are extracted: density ratio (x36), number of nodes (x37) and number of links or edges (x38).

2.3.4.Texture Features

Vascular pattern, blue-gray veil, white scar like areas, and dots or globules, these structures are usually associated with texture features. Vascular pattern is associated to the presence of a vascular vessel with line shape, and gray-blue areas and white scar-like areas are found as homogeneous areas.

1. Gray Level Co-Occurrence Matrix (GLCM):

The gray level co-occurrence matrix is considered, given its effectiveness in pigmented lesion classification. It counts how often a pixel with gray intensity of i occurs adjacent to a pixel with gray intensity of j. Therefore, it is necessary to convert the original RGB image into a grayscale image. We select the color channel of the RGB image with the highest entropy. The images are uniformly quantized to 64 gray levels, as previously proposed [19], and the GLCM is computed for four different orientations of {0, 45, 90,180}. Finally, the statistics calculated from these matrices were averaged. For each orientation, 19 statistical texture descriptors were extracted and then averaged (x39-x57)

2 Markov Random Fields (MRF):

A model based on Markov random fields is used to extract texture features to identifying different dermoscopic structures. The intensity at each pixel depends on the neighboring pixels intensity. Finally, obtain 18 parameters (x58-x75).

3. Local Binary Pattern(LBP):

Local binary pattern (LBP) histograms is used for the characterization of texture in pigmented lesions. This

method labels the pixels of an image by thresholding the neighborhood of each pixel based on its value and generates a number to quantify the local texture. A histogram is used to describe the texture information of the whole lesion. . Then compute LBP features over the same channel that was computed the GLCM, using eight sampling points on a circle of radius R=2 and R=10. Three statistics (SD, Ku and Sk) over the two LBP histograms are extracted.

2.4 Classification

Main aim is to classify the various stages of skin cancer. Here use two different classification methods. First one is binary classification method where find the two stages in skin cancer. They are thin and thick stages. In the second classification method find the three stages of cancer they are thin, intermediate and thick stages. The classification is based on kernel nearest neighbour (KNN).The idea behind the k-Nearest Neighbour algorithm is to build a classification method using no assumptions about the form of the function, y = $f(x_1,x_2,...x_p)$ that relates the dependent (or response) variable, y, to the independent (or predictor) variables $x_1,x_2,...x_p$. The only assumption we make is that it is a"smooth" function. This is a non-parametric method because it does not involve estimation of parameters in an assumed function form such as the linear form that encountered in linear regression. Use a training data in which each observation has a y value which is just the class to which the observation belongs. For example, if we have two classes y is a binary variable. The idea in k-Nearest Neighbour methods is to dynamically identify k observations in the training data set that are similar to a new

observation , say (u_1,u_2,...u_p), that we wish to classify and to use these observations to classify the observation into a class, v. If we knew the function f, we would simply compute v = f(u_1,u_2,...u_p). If all we are prepared to assume is that f is a smooth function, a reasonable idea is to look for observations in our training data that are near it (in terms of the independent variables) and then to compute v from the values of y for these observations. This is similar in spirit to the interpolation in a table of values that we are accustomed to doing in using a table of the Normal distribution. When we talk about neighbours we are implying that there is a distance or dissimilarity measure that we can compute between observations based on the independent variables. For the moment we will confine ourselves to the most popular measure of distance: Euclidean distance. The Euclidean distance between the points (x_1,x_2,...x_p) and (u_1,u_2,...u_p) is $(x_1 - u_1)^2 + (x_2 - u_2)^2 + \cdots + (x_p - u_p)^2$. We will examine other ways to define distance between points in the space of predictor variables when we discuss clustering methods. The simplest case is k = 1 where we find the observation that is closest (the nearest neighbour) and set v = y where y is the class of the nearest neighbour. It is a remarkable fact that this simple, intuitive idea of using a single nearest neighbour to classify observations can be very powerful when we have a large number of observations in our training set.

3. Experimental Procedure

3.1Performance Evaluation and Experimental Design

Table 2:Performance of class three problem

Three Class Problem			
Method	Acc	MS	AMAE
LIPU	.684	.185	.656
LR	.632	.069	.813
PUNN	.648	.148	.759
KNN	.644	.552	.449
SVC	.664	.259	.675

Performance evaluation of classification tasks is a multidimensional issue, and model behaviour assessment depends on the specific problem requirements. In our case, we have selected the following classification performance metrics based on the application purpose:

• Accuracy (Acc) is the rate of correctly classified patterns and represents the global performance of the classification task:

$$Acc = \frac{1}{N} \sum_{i=1}^{N} [|\hat{y}_i = y_i|], \qquad (2)$$

Where $[|c|]$ is the indicator function, being equal to 1 if c is true, and to 0 otherwise. Acc values range is [0,1]. Minimum Sensitivity (MS) is proposed to measure imbalanced multi-class models performance, and it is defined as the minimum per class Sensitivity (Si): MS = min {Si; i = 1,...,J}, where J is the number of classes, and Si is the accuracy taking into account only patterns from class Ci. Mean Absolute Error (MAE) is the average deviation in absolute value of the predicted class from the true class. For imbalanced datasets, this measure should be modified to consider the relative frequency of the classes, deriving in the Average MAE (AMAE):

$$AMAE = \frac{1}{j} \sum_{j=1}^{J} MAE_j = \frac{1}{j} \sum_{q=1}^{J} \frac{1}{n_q} \sum_{i=1}^{n_q} e(x_i) \qquad (3)$$

where $e(x_i) = |o(y_i) - o(\hat{y}_i)|$ is the distance between the true and the predicted ranks, $O(C_q) = q$ is the position of the q^{th} label, n_q is the number of patterns of class Cq, and AMAE values range from 0 to J −1. For the binary case, AMAE can be seen as a Weighted Accuracy (WAcc), because the errors (e(xi)) will be 0 or 1. Experiments are performed using a 10-fold cross-validation. All the features were properly standardized using mean and variance of the training data of each fold. The parameter values for LIPU and PUNN algorithms can be found .To adjust the hyper-parameters of the rest of methods, a nested cross validation is applied to the training data, with a grid search for the different values. The criteria for selecting the parameters is AMAE or WAcc.

3.2.Experimental Results

Experimental results are presented in terms of generalization performance of the models in Table 2. The different metrics are obtained from the sum of the 10 unseen predictions done by each method in the 10-fold setup. A public website with the dataset and 10 partitions together with links to implementations of all the methods used in the experiments, as well as supplementary materials are provided. In addition, Table 3 shows generalization confusion matrices for LIPU

And KNN to complement performance analysis. The matrices for the remaining methods are included as supplementary data in the website associated to this paper. For the binary case, the LIPU has the best performance in Acc and AMAE, and the second best performance in MS. For the ordinal classification problem, LIPU has the best Acc; On the other hand, KNN has the best performance in MS and AMAE for the ordinal problem, achieving a 55.2% of accuracy for the worst classified class (C3), with a mean error magnitude below 0.5 of distance (in number of categories) between the true and predicted class. Note the performance of the LR and PUNN is

improved by LIPU model in all the cases, but here KNN classifiers is better compared to the others. Finally, observe that the nominal methods have the worst performance if we consider AMAE[17].

Table 3::Experimental results in mean considering three classification performance metrics

Binary problem			
Method	Acc	MS	W Acc
LIPU	.766	.602	.268
LR	.752	.530	.304
PUNN	.720	.494	.337
KNN	.712	.663	.300
SVC	.764	.518	.298

Table 4: LIPU and KNN in the binary and ordinal databases.

Binary Problem					
LIPU			KNN		
	thin	Rest		Thin	Rest
Thin	144	23	Thin	123	44
Rest	33	50	Rest	28	55

Three class problem							
LIPU				KNN			
	Thin	Interm.	Thick		Thin	Interm.	Thick
Thin	154	12	1	Thin	115	47	5
Interm.	40	10	4	Intrm.	19	30	5
Thick	9	13	7	Thick	3	10	16

4. CONCLUSION

By using KNN here performed feature selection during the learning phase. All features included in this model were either in the linear part or non-linear part of the model. However, some features has a greater relevance because they are included individually in the majority of the models. This is the case of features related to black and blue colors, pigment network, homogeneity and some texture features extracted from three approaches proposed. , in our system the shape features, red color associated to vascular pattern and white color associated to white scar-like areas were more important, these features do not have an individual influence in the linear part, although they do interact with others on the basis functions.

Next proposed a three-class scheme, in which melanoma is classified into three stages. This second approach is motivated by the fact that the melanoma depth is correlated with the patients survival, and therefore, a finest estimation of tumor thickness will lead to a more accurate diagnosis. Ordinal classification is performed due to the complexity, which assume the natural ordering between the melanoma types, improved performance and reduce the magnitude of classification errors. These type of methods are applied to a pigmented lesion recognition problem. The results show that an ordinal method achieves a better balance between the performances obtained for all classes and reduces the magnitude of the errors in such a way that, when patterns are misclassified, the label predicted is as close as possible to the real label. This method achieved an average 99.9

REFERENCES

[1] M. Pizzichetta *et al.*, "Dermoscopic criteria for melanoma in situ are similar to those for early invasive melanoma," *Cancer*, vol. 91, no. 5, pp. 992–997, 2001.

[2] S. Baccianella, A. Esuli, and F. Sebastiani, "Evaluation measures for ordinal regression," in Proc. 9th IEEE Comput. Soc. Int. Conf. Intell. Syst. Design Appl., San Mateo, CA, 2009, pp. 283–287.

[3] A. Kardynal and M. Olszewska, "Modern non-invasive diagnostic techniques in the detection of early cutaneous melanoma," *J. Dermatol. Case Rep,*, vol. 8, no. 1, pp. 1–8, 2014

[4] B.-Y. Sun, J. Li, D. D. Wu, X.-M. Zhang, and W.-B. Li, "Kernel discriminant learning for ordinal regression," *IEEE Trans. Knowl. Data Eng.*, vol. 22, no. 6, pp. 906–910, Jun. 2010.

[5] A. Breslow, "Thickness, cross-sectional areas and depth of invasion in the prognosis of cutaneous melanoma," *Ann. Surg.*, vol. 172, no. 5, pp. 902–908, 1970.

[6] M. Amouroux and W. Blondel, M. Y. Cao, Ed., "Non-invasive determination of Breslow index," Current Manage. Malignant Melanoma InTech, pp. 29–44 [Online]. Available: https://hal.archives-ouvertes.fr/ hal-00626482

[7] M. Stante, V. De Giorgi, P. Cappugi, B. Giannotti, and P. Carli, "Noninvasive analysis of melanoma thickness by means of dermoscopy: A retrospective study," *Melanoma Res.*, vol. 11, no. 2, pp. 147–152, 2001.

[8] M. B. Lens, P. Nathan, and V. Bataille, "Excision margins for primary cutaneous melanoma: Updated pooled analysis of randomized controlled trials," *Arch. Surg.*, vol. 142, no. 9, pp. 885–891, 2007.

[9] P. Rubegni *et al.*, "Evaluation of cutaneous melanoma thickness by digital dermoscopy analysis: A retrospective study," *Melanoma Res.*, vol. 20, no. 3, pp. 212–217, 2010.

[10] P. Cavalcanti and J. Scharcanski, "Texture information in melanocytic skin lesion analysis based on standard camera images," in Comput. Vision Techniques for the Diagnosis of Skin Cancer, J. Scharcanski and M. E. Celebi, Eds. Berlin, Germany: Springer, 2014, pp. 221–242

[11] D. Rigel, J. Russak, and R. Friedman, "The evolution of melanoma diagnosis: Years beyond the abcds," *CA Cancer J. Clin.*, vol. 60, no. 5, pp. 301–316, 2010.
[12] M. Vestergaard, P. Macaskill, P. Holt, and S. Menzies, "Dermoscopy compared with naked eye examination for the diagnosis of primary melanoma: A meta-analysis of studies performed in a clinical setting," *Brit. J. Dermatol.*, vol. 159, no. 3, pp. 669–676, 2008.
[13] A. Gulia and C. Massone, Advances in dermoscopy for detecting melanocytic lesions F1000 Med. Rep., 2012, vol. 4.
[14] P. Carli, V. De Giorgi, D. Palli, V. Giannotti, and B. Giannotti, "Preoperative assessment of melanoma thickness by ABCD score of dermatoscopy," *J. Am. Acad. Dermatol.*, vol. 43, no. 3, pp. 459–466, 2000.
[15] R. Garnavi, M. Aldeen, and J. Bailey, "Computer-aided diagnosis of melanoma using border- and wavelet-based texture analysis," *IEEE Trans. Inf. Technol. Biomed.*, vol. 16, no. 6, pp. 1239–1252, Nov. 2012. [19] M. Celebi *et al.*, "A methodological approach to the classification of dermoscopy images," *Comput. Med. Imag. Graph.*, vol. 31, no. 6, pp. 362–373, 2007.
[16] G. Argenziano, G. Fabbrocini, P. Carli, V. De Giorgi, and M. Delfino, "Clinical and dermatoscopic criteria for the preoperative evaluation of cutaneous melanoma thickness," *J. Am. Acad. Dermatol.*, vol. 40, no. 1, pp. 61–68, 1999.
[17] H. Lorentzen, K. Weismann, and F. Grnhj Larsen, "Dermatoscopic prediction of melanoma thickness using latent trait analysis and likelihood ratios," *Acta Dermato-Venereologica*, vol. 81, no. 1, pp. 38–41, 2001.
[18] G. Argenziano *et al.*, "Blue-black rule: A simple dermoscopic clue to recognize pigmented nodular melanoma," *Br. J. Dermatol.*, vol. 165, no. 6, pp. 1251–1255, 2011.
[19] V. da Silva, J. Ikino, M. Sens, D. Nunes, and G. Di Giunta, "Dermoscopic features of thin melanomas: A comparative study of melanoma in situ and invasive melanomas smaller than or equal to 1 mm, caractersticas dermatoscpicas de melanomas finos: Estudo comparativo entre melanomas in situ e melanomas invasivos menores ou iguais a 1 mm," *Anais Brasileiros de Dermatologia*, vol. 88, no. 5, pp. 712–717, 2013.
[20] I. Maglogiannis and C. N. Doukas, "Overview of advanced computer vision systems for skin lesions characterization," *IEEE Trans. Inf. Technol. Biomed.*, vol. 13, no. 5, pp. 721–733, Sep. 2009.